

We are IntechOpen, the world's leading publisher of Open Access books Built by scientists, for scientists

6,900

Open access books available

186,000

International authors and editors

200M

Downloads

Our authors are among the

154

Countries delivered to

TOP 1%

most cited scientists

12.2%

Contributors from top 500 universities



WEB OF SCIENCE™

Selection of our books indexed in the Book Citation Index
in Web of Science™ Core Collection (BKCI)

Interested in publishing with us?
Contact book.department@intechopen.com

Numbers displayed above are based on latest data collected.
For more information visit www.intechopen.com



Chitosan: Strategies to Increase and Modulate Drug Release Rate

David Lucio and María Cristina Martínez-Ohárriz

Additional information is available at the end of the chapter

<http://dx.doi.org/10.5772/65714>

Abstract

Chitin is the second most abundant polysaccharide present in nature; however, chitin has more applications when transformed into chitosan (CS). It is biocompatible, biodegradable, mucoadhesive, soluble in acidic-solutions, nontoxic and nonallergenic. The main drawback of chitosan in pharmaceutical procedures is its low solubility in physiological medium. Chitosan shows physicochemical characteristics that allow it to interact with a wide variety of molecules. This is of particular interest when increasing the solubility of poor water-soluble drugs. For this purpose, chitosan can be used in oral, nasal and ocular routes. In order to modulate drug release rate and achieve a proper drug delivery in physiological medium, some parameters can be modified when solid dispersions or nanoparticles (NPs) based on chitosan are being designed. In case of nanoparticles, chitosan can be used as the main component or as a modifying agent. In order to optimize drug loading and drug delivery, response surface methodology (RSM) is an interesting tool usually underestimated in the pharmaceutical field, which allows us to optimize the parameters involved in the process simultaneously and not by different steps, which usually lead to mistakes.

Keywords: chitosan, carboxymethyl chitosan, drug delivery, nanoparticles, solid dispersions, porous microstructure, response surface methodology

1. Introduction

Chitin is the second most abundant polysaccharide and the only cationic one present in nature; these characteristics make it suitable and interesting for industrial uses [1]. However, chitin has more applications when transformed into chitosan (CS) by partial deacetylation under alkaline conditions [2].

Chitosan [(1-4)-2-amino-2-deoxy- β -D-glucan] is a linear cationic polysaccharide comprising by N-acetyl glucosamine and glucosamine units (**Figure 1**). Although research is more advanced in the case of cellulose, amino groups provide an important advantage to chitosan due to its ease to be chemically modified, including functional groups that would give new properties for more specific uses [3, 4].

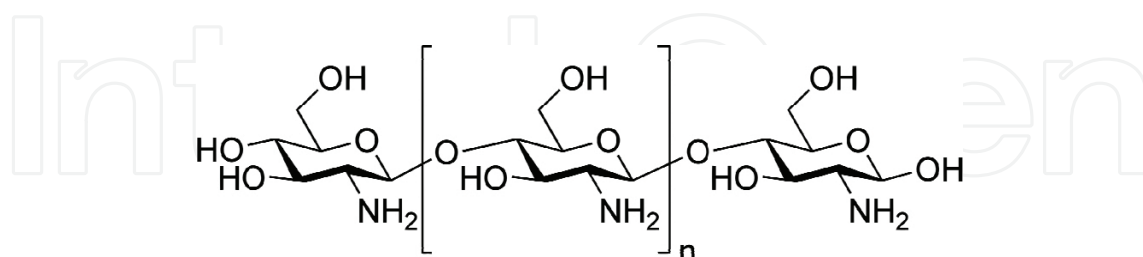


Figure 1. Representation of chitosan molecule.

Chitosan are receiving increasing attention in the industrial domain as a consequence of their special properties. It is a biocompatible, biodegradable, mucoadhesive, and transmucosal penetration enhancer, soluble in acidic solutions, nontoxic and nonallergenic [5]. Moreover, because it is generally recognized as safe (GRAS), which together with its abundance and low cost make chitosan a particularly interesting material for its use in the pharmaceutical field [6, 7]. In addition, its antacid and antiulcer activities made chitosan and its derivatives an interesting alternative if gastric irritation wants to be avoided when anti-inflammatory drug are administered [8, 9]. Finally, chitosan is an excellent direct compression adjuvant, an important characteristic for potential pharmaceutical formulations [10].

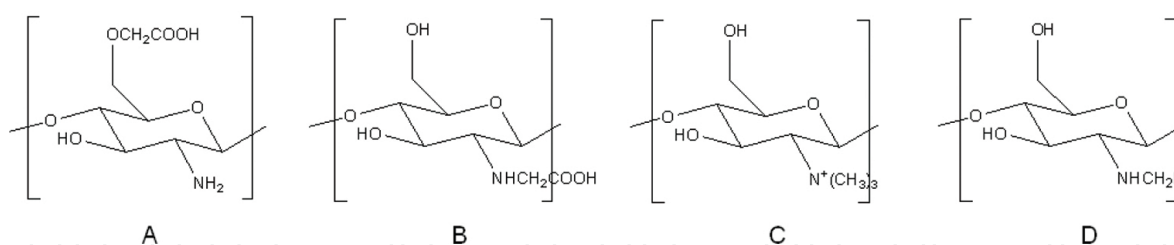


Figure 2. Representation of molecules of O-carboxymethyl chitosan (A), N-carboxymethyl chitosan (B), trimethyl chitosan (C), and N-alkyl chitosan (D).

The main drawback of chitosan in pharmaceutical procedures is its low solubility in aqueous solutions and physiological medium [11, 12]; acetylation degree and molecular weight are the most relevant variables which condition chitosan solubility [13]. However, this problem can be solved, thanks to the easy modification of its primary aliphatic amine group. This fact allows us to obtain water-soluble derivatives such as carboxymethyl chitosan, trimethyl chitosan, and N-alkyl chitosans (**Figure 2**) [14]. Both chitosan and its derivatives have physicochemical characteristics that allow them to interact with a wide variety of drugs. This is of particular interest when trying to increase the solubility of poor water-soluble drugs [15, 16], which is a

fundamental strategy to increase low bioavailability of drugs belonging to Groups II (low solubility, high permeability) and IV (low solubility, low permeability) of Biopharmaceutical Classification System (BCS). In this sense, different strategies have been developed to increase the solubility of these drugs, such as particle size reduction, drug fusion and preparation of solid dispersions, nanosuspensions, amorphous states, inclusion complexes, or nanoparticles (NPs).

For this purpose, chitosans can be used in oral, nasal, and ocular routes, being the first one considered as the safest and most advisable way. Drug-controlled release by oral route has been achieved using chitosan in several pharmaceutical dosage forms such as solid dispersions, cross-linked hydrogels or nanoparticles [17, 18]. In case of nanoparticles, chitosan can be used both as modifying agent and as the main component by different methods such as cross-linking, ionic gelation, or solvent evaporation.

As it is well known, drug delivery from polymeric systems is influenced by several factors: polymer molecular weight, deacetylation and substitution degree of polysaccharides, nanoparticle size, porous structure, or compression force are some of the factors which directly determine the release rate from a solid matrix. The length and conformation of polysaccharide chains influence the accessibility of chitosan functional groups by drug molecules, which is crucial to establish electrostatic interactions and the subsequent incorporation of drug molecules into these systems.

Furthermore, different preparation methods can lead to different interactions and porous structures when nanoparticles are formed or tablets are prepared by compression [19]. Porous microstructures (pore size distribution, porosity, tortuosity, etc.) strongly affect the penetration of solvent into matrixes, dissolution of drug molecules, and subsequent release of these molecules to the medium. This fact can be observed when the release rate studies were conducted for similar systems but different porous structures as consequence of preparation method.

In these pharmaceutical processes, there are some parameters which can be modified with the typical aims to incorporate the maximum amount of drug into the systems or to achieve a proper drug delivery in physiological medium. In order to optimize these characteristics, design of experiments is an interesting tool usually underestimated in the pharmaceutical field; however, recently, it is being considered a point of interest to maximize the benefits of some processes. Simplifying the process, reducing the economic cost, and improving the characteristics of the final formulation are key features that can make a formulation cross the barrier from laboratory to market. For this purpose, response surface methodology (RSM) has proven to be a suitable tool when trying to optimize a procedure [20]. This strategy is especially interesting when the response to be optimized is influenced by two or more parameters simultaneously or when two different responses must be optimized at the same time.

It is worthy to note that one of the most common mistakes when a response is being optimized is trying to modify each parameter independently. All individual parameters may produce a determined variation in the response depending on the specific value taken by the other

influential parameters. For this reason, this parameter modification should be done simultaneously and not individually.

In the past, our group has explored the use of different polymers such as PEG [21], PVP [22], poly(anhydride) [23], chitosans [18], or cyclodextrins [24, 25] to obtain systems, which can increase the bioavailability of different drugs. To improve the properties of these delivery systems, along with the drug of interest, various polymers can be combined to provide improvements in several properties, such as the drug solubility increase and the achievement of a controlled release system at the same time.

The aim of the current chapter was to investigate the possibilities and advantages of chitosan-based system for the oral administration of drugs, which show low bioavailability as consequence of its low solubility in different dosage forms: tablets and nanoparticles. Diflunisal (DF) has been chosen as model molecule (**Figure 3**). It is a drug with analgesic and anti-inflammatory activity, and it has been shown to interact with a high variety of polymers [26].

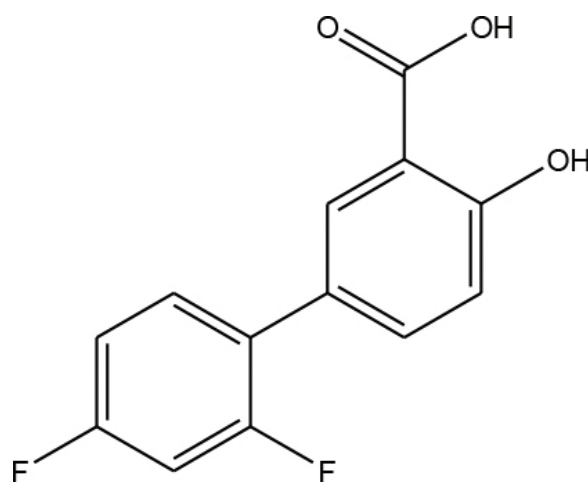


Figure 3. Representation of diflunisal molecule.

2. Materials and methods

2.1. Materials

Diflunisal (DF) was kindly supplied by Merck Sharp and Dohme (Spain). Chitosan (>375 kDa) was supplied by Sigma-Aldrich with a degree of deacetylation of 75–85%. 2-(Hydroxypropyl)- β -cyclodextrin (HP β CD) was purchased from Cyclolab (Hungary). Hydroxypropyl methylcellulose (HPMC) K4M was obtained from Colorcon (Orpington, UK), and sodium alginate (Alg) was supplied by Sigma-Aldrich. The reagents ethanol (Scharlau, PA), ammonium hydroxide, and hydrochloric acid (Panreac, analytical grade) were used as received. All aqueous solutions were prepared with deionized water obtained from a commercial Millipore Elix 3 system (0.1 μ S/cm conductivity).

2.2. Preparation of solid dispersions

Diflunisal-chitosan solid dispersions were prepared by kneading at 20:80 drug/polymer ratio. Chitosan was wetted in a mortar with a minimum volume of an ethanol/water solution (50%, v/v) and kneaded with a pestle, while diflunisal was added until a dense paste was formed.

2.3. Preparation of nanoparticles

Chitosan-based nanoparticles can be easily formed via ionic gelation due to the interaction between the positive charges of chitosan amine groups and negative charges of sulfate ions. In order to incorporate the maximum amount of drug into nanoparticles, inclusion complexes with cyclodextrins were previously formed by a coevaporation method.

Chitosan- and drug-cyclodextrin complexes were dissolved in water and added over an aqueous solution containing sodium sulfate (SS). After the immediate formation by ionic gelation, nanoparticles were centrifugated at $20,000 \times g$, frozen, and then freeze-dried.

2.4. Optimization of nanoparticles: response surface methodology

The effective parameters in the NP formation process, including CS, sodium sulfate, and DF-HP β CD complex concentrations were optimized using response surface methodology. Statgraphics Centurion XVI.I software was used in order to find the best combination of factors which minimize nanoparticle diameter and polydispersity index (PDI) simultaneously. Central composite design (CCD) was chosen due to its orthogonal and rotatable properties. It is also an appropriate design of experiments when a process is influenced by more than two factors at the same time because of the reduction of the experiment number:

$$\text{Number of experiments} = 2^n + 2 \cdot n + \text{central point replicates} \quad (1)$$

where n is the number of factors involved in the process optimization.

2.5. Characterization techniques

2.5.1. X-ray diffractometry (XRD)

X-ray powder diffraction patterns were collected on a X Bruker axs D8 Advance diffractometer (Karlsruhe, Germany) using a CuK_α radiation.

2.5.2. Scanning electron microscopy

The shape and surface morphology were examined by scanning electron microscopy (SEM) (Zeiss DSM 940 A apparatus) provided with a digital image capture system (DISS de Point Electronic GmbH).

2.5.3. Transmission electron microscopy (TEM)

The morphology and size of nanoparticles in water solution were analyzed using a transmission electron microscope (TEM). Samples were analyzed using a LIBRA 120 energy-filtering TEM (Zeiss) operated at 80 kV.

2.5.4. Dynamic light scattering

The size distribution of nanoparticles was determined by dynamic light scattering (DLS) using a DynaPro photon correlation spectrometer at $25.0 \pm 0.1^\circ\text{C}$. The intensity of size distributions, expressed in terms of the hydrodynamic radius (R_h), was calculated by the Stokes-Einstein equation:

$$R_h = \frac{kT}{6\pi\eta_0 D_0} \quad (2)$$

2.5.5. Zeta potential

The zeta potential of nanoparticles was measured by electrophoretic laser Doppler anemometry using a Zetamaster analyzer system (Malvern Instruments, UK).

2.6. Dissolution rate studies

The in vitro dissolution studies of pure drug and tablets including solid dispersions were performed using tablets containing 150 mg of diflunisal-chitosan solid dispersions. These dispersions were pressed on an instrumented single-punch tablet press (Kilian SP300, IMA, Germany) using round flat-faced punches (7 mm diameter and 3.15 mm thickness). HPMC and sodium alginate were added directly before the compression process.

The dissolution rate assays were performed in a SOTAX AT 7smart (SOTAX, Basel, Switzerland) tablets, or NPs were placed in 900 mL of PBS (Phosphate Buffer Solution) 7.4 medium at 37.0°C and stirred at 50 rpm.

3. Results and discussion

3.1. Optimization of nanoparticle formation process

Nanoparticles were easily formed via ionic gelation due to the interactions between positive charges of chitosan and negative charges of sodium sulfate.

Optimization of particle size was carried out using response surface methodology and central composite design of experiments. In previous experiments, several characteristics of the process were studied. Nanoparticles were formed using chitosan of high, medium, and low

molecular weight; high molecular weight was the most suitable material because the chain length is longer, and this fact facilitates folding and therefore the nanoparticle formation when contact to the negative charges of sodium sulfate. The volume of solutions employed and stirring rate were shown to be non-influential factors in the process. **Table 1** shows factors to optimize particle size and polydispersity index responses.

Factors			Responses	
Chitosan (%)	HP β CD-DF (%)	Sodium sulfate (%)	NP size (nm)	PDI
0.3	0.3	3	821	0.201
0.3	0.3	3	813	0.175
0.3	0.3	3	788	0.234
0.3	0.3	3	801	0.197
0.3	0.3	3	801	0.185
0.5	0.5	5	5217	0.721
0.3	0.3	6.4	2415	0.485
0.3	0.0	3	1851	0.258
0.3	0.3	3	783	0.414
0.3	0.3	3	797	0.294
0.3	0.3	3	846	0.215
0.1	0.5	5	697	0.109
0.3	0.3	0	–	–
0.3	0.3	3	825	0.253
0.5	0.5	1	3655	0.449
0.5	0.1	1	504	0.263
0.1	0.1	5	1290	0.503
0.1	0.5	1	505	0.432
0.64	0.3	3	1002	0.218
0.5	0.1	5	1454	0.298
0.3	0.64	3	3811	0.516
0.1	0.1	1	488	0.218
0.0	0.3	3	–	–

Table 1. Experiments corresponding to the central composite design study.

Analysis of variance (ANOVA) for particle size and polydispersity index allows us to identify which factors and interactions between factors influence the responses. Pareto chart indicates the statistically significant factors in order to build the response surface mathematical model

(Figure 4). Subsequently, the mathematical model can be built to predict the response depending on the value taken by the factors.

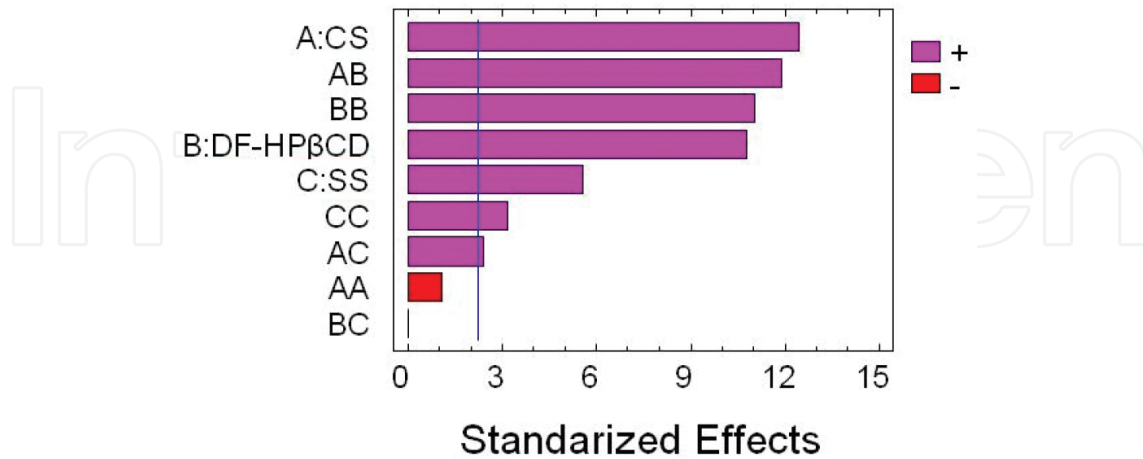


Figure 4. Pareto chart (Factor A = chitosan concentration, Factor B = complex concentration, and Factor C = sodium sulfate concentration).

The model obtained for the optimization of particle diameter explains 98.3% of the variability in the experimental data, whereas for the optimization of polydispersity index, the model obtained explains only 88% of the variability of experimental data. **Figure 5** shows a schematic representation of the response surface for a pair of factors influencing the particle size.

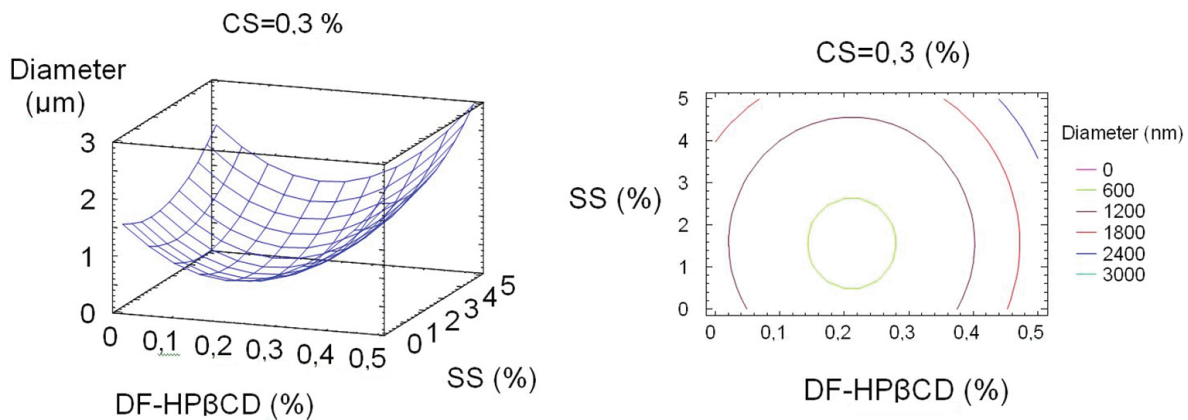


Figure 5. Schematic representation of response surface for particle diameter as a function of DF-HPβCD and sodium sulfate concentration (variation in the third factor cannot be shown in the same figure; for this reason, chitosan concentration has been set on 0.3%).

The three-dimensional representation of the response as a function of two factors (**Figure 4**) does not allow us to visualize the minimum value for the selected surface. **Figure 6** allows us to carry out a preliminary analysis of the influence of each individual factor and its interactions in the response.

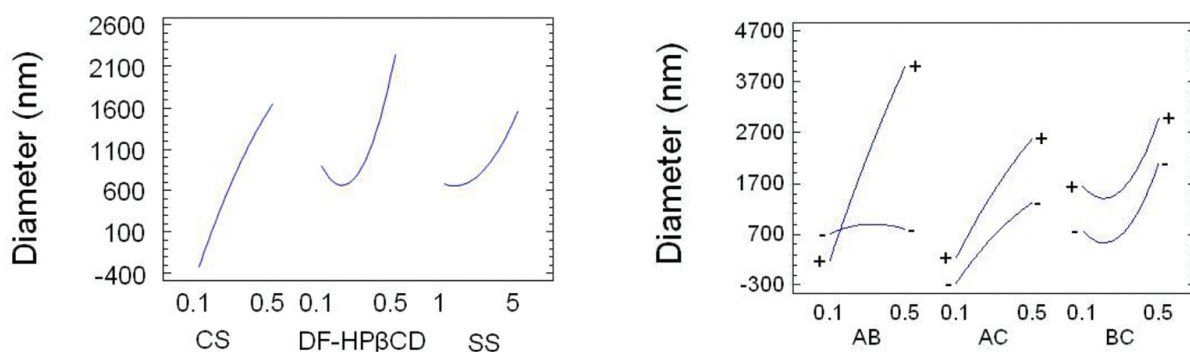


Figure 6. Schematic representation of the influence of each factor and the interactions between factors in the particle diameter (Factor A = chitosan concentration, Factor B = complex concentration, and Factor C = sodium sulfate concentration).

The minimum particle diameter was obtained for concentrations of chitosan 0.12%, DF-HPβCD 0.34%, and sodium sulfate 2.2% according to the prediction of the mathematical model. Moreover, the minimum polydispersity index was obtained for concentrations of chitosan 0.61% and sodium sulfate 1.2% (DF-HPβCD concentration is not an influence factor for PDI).

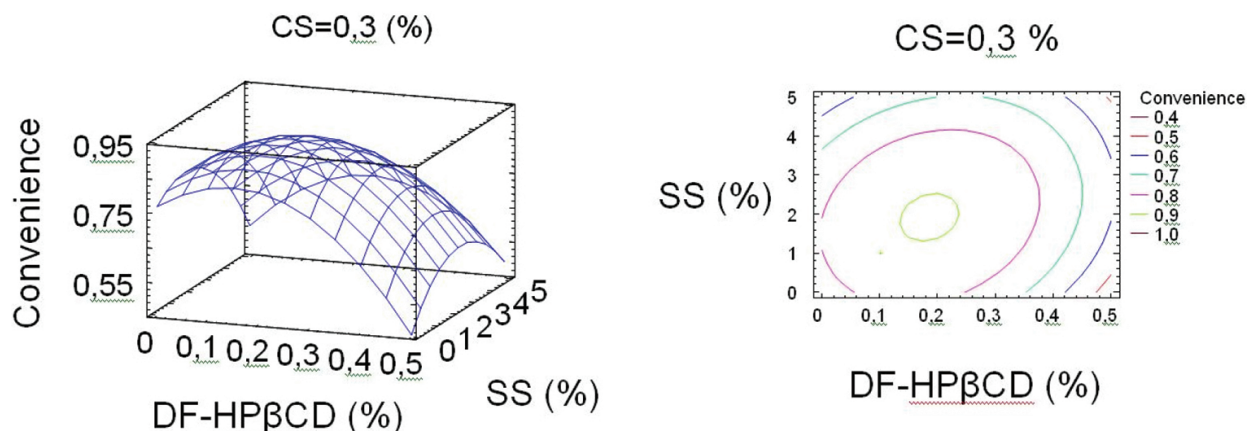


Figure 7. Schematic representation of response surface for convenience of responses as a function of DF-HPβCD and sodium sulfate concentration (variation in the third factor cannot be shown in the same figure; for this reason, chitosan concentration has been set on 0.3%).

As can be observed, the optimization of both responses leads to different values for the three factors. It is therefore necessary to define a new function that optimizes the convenience of both responses simultaneously. For that purpose, a weight three times greater was conferred for the particle diameter than for polydispersity index. The representation of the response surface desirability function is shown in **Figure 7**. The values of factors for obtaining the best nanoparticles in terms of particle diameter and polydispersity index simultaneously are chitosan 0.14%, DF-HPβCD 0.28%, and sodium sulfate 1.9%.

Once the model that describes the function convenience was built, the nanoparticles were performed using the optimal conditions calculated showing a particle diameter of 515 nm and

a polydispersity index of 0.14. The optimized nanoparticles showed a formation yield of 72.6%, an encapsulation efficiency of 34% and the amount of drug encapsulated was 42.3 $\mu\text{g}/\text{mg}$.

3.2. Characterization of nanoparticles

After the optimization from based on response surface methodology, physicochemical characterization of the optimized formulation was carried out.

It is important to ensure that all drug molecules are contained inside the nanoparticle and not distributed on the surface in order to prevent releases in two stages when it is intended to obtain controlled release systems [27]. With the aim to verify the distribution of drug in these systems, X-ray powder diffractometry was carried out (**Figure 8**). The absence of drug crystals on nanoparticle surface was corroborated, so a release in one single mode could be expected.

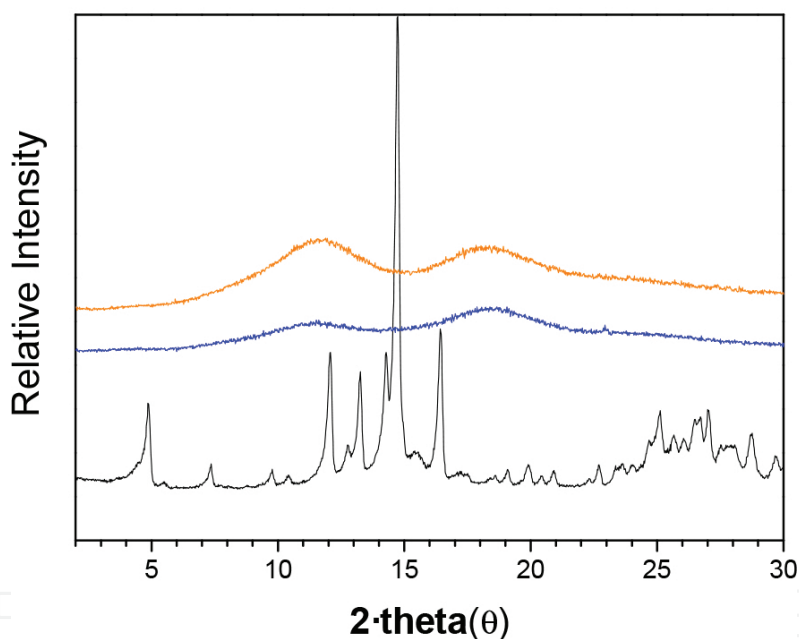


Figure 8. X-ray diffraction patterns of diflunisal (—), chitosan empty nanoparticles (—), and optimized nanoparticle formulation CS-(DF-HP β CD) (—).

The study of nanoparticle morphology was carried out by transmission electron microscopy. Round shape of nanoparticles can be visualized in **Figure 9**, confirming the previously measured particle size by dynamic light scattering (DLS), which reported a particle diameter distribution between 500 and 550 nm. The size measured by DLS is slightly higher than shown in the TEM images. This fact is due to the measurements of hydrodynamic radius obtained by DLS (which include solvent molecules displaced together with solid nanoparticles) and is always higher than the real size of nanoparticles. The zeta potential of the systems was 33.2 mV ensuring the stability of the nanoparticles in solution.

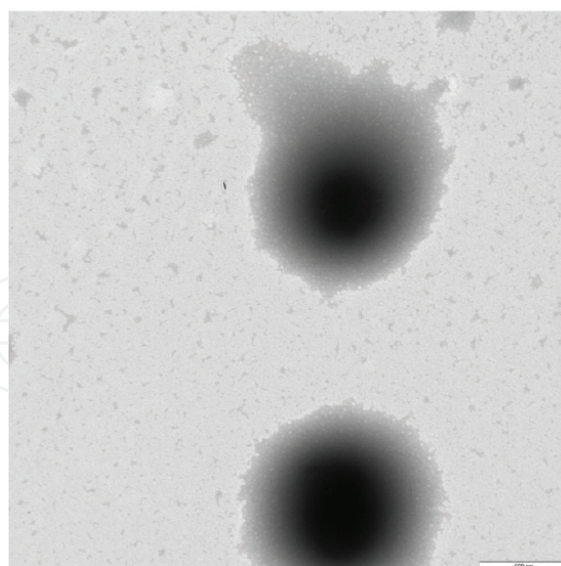


Figure 9. TEM image of the optimized nanoparticle formulation CS-(DF-HP β CD).

3.3. Characterization of solid dispersion systems

Diffenlunisal and chitosan solid dispersions were analyzed by X-ray diffractometry (XRD) and scanning electron microscopy (SEM). It is important to characterize the crystalline state of drug molecules if it will be administered by oral route. Drugs in crystalline state usually show a lower dissolution rates, because it is necessary to use a certain amount of energy to break the crystal lattice formed by drug molecules.

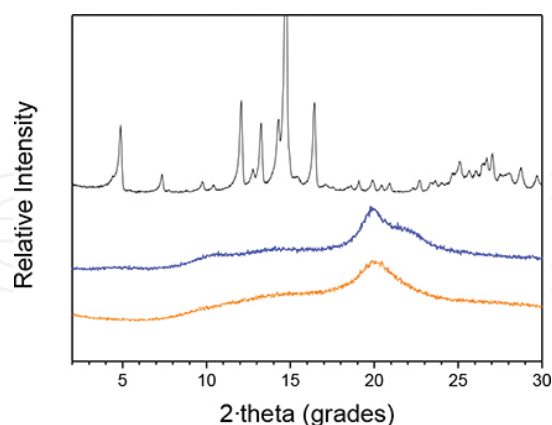


Figure 10. XRD patterns of diflunisal (—), DF-CS kneaded system (—), and chitosan (—).

The X-ray diffraction patterns of pure components, diflunisal and chitosan, and DF-CS-kneaded systems are shown in **Figure 10**. Chitosan shows the typical profile of amorphous materials. Diflunisal diffraction pattern showed the peaks of polymorph II [28, 29]. The kneading of diflunisal and chitosan gave rise to amorphous systems, and the X-ray diffraction

pattern showed the absence of reflections as a consequence of the breaking of crystal lattice formed by molecules of diflunisal, which is molecularly dispersed within the amorphous polymer.

SEM micrographs show diflunisal as long prismatic, rodlike crystals typical of crystalline form II [19]. Chitosan particles showed rough surface with very different particle sizes. The disappearance of diflunisal needle agglomerates when the complex was observed corroborates the interaction between drug and polymer (**Figure 11**).

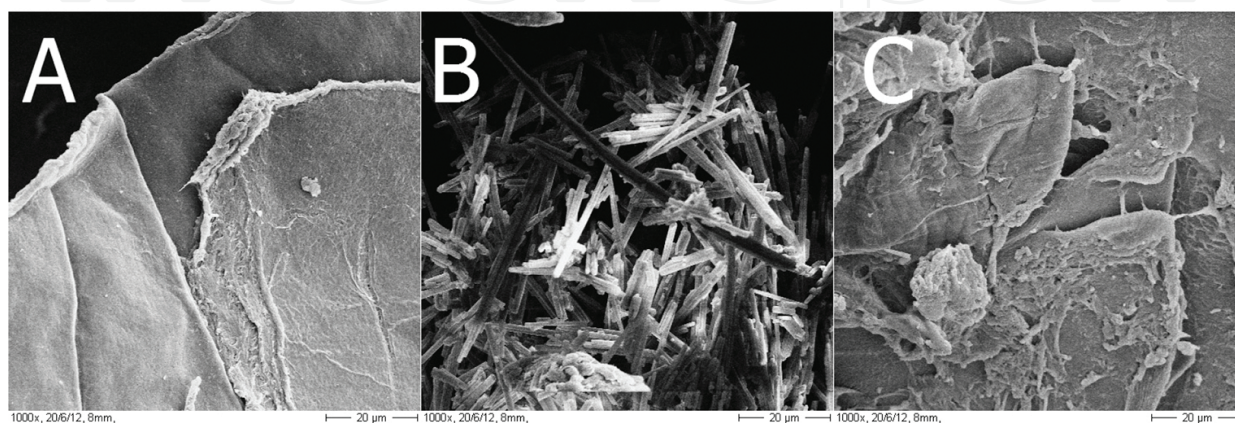


Figure 11. SEM micrographs of chitosan (A), diflunisal (B), and DF-CS-kneaded system (C).

3.4. Dissolution rate studies

3.4.1. Dissolution from tablets

Drug solubility enhancement caused by interaction with chitosan has been described previously in the literature [19]. The interaction by hydrogen bonds between diflunisal and chitosan is the main reason by which a faster release of diflunisal can be expected when it is compressed in the presence of chitosan. Different agents commonly used in the pharmaceutical industry have been employed to modulate diflunisal release rate from solid dispersions formed with chitosan by kneading. The dissolution rates from the different matrices prepared are shown in **Figure 12**.

Diflunisal release from tablets formed by kneading with chitosan showed a very fast release of diflunisal; in this case, the maximum amount of diflunisal was released to the medium in less than 1 h. In order to modulate drug release rate, it is therefore necessary to employ agents able to delay drug delivery. Sodium alginate and hydroxypropyl methylcellulose are widely used in the pharmaceutical domain for this purpose. These agents cause matrix gelification in aqueous solution promoting the slowly release of drug by diffusion from inside the matrix. For both concentrations of alginate, the plateau was reached at 15 h; in case of the addition of HPMC, the complete drug release was not achieved until 30 h, thereby achieving a much slower release.

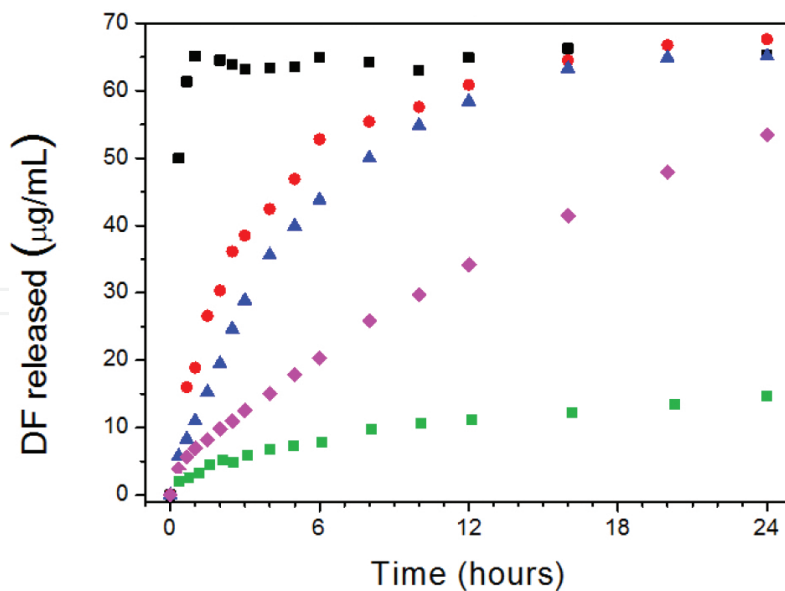


Figure 12. Dissolution rate of diflunisal from tablets compressed DF-CS systems alone (■) or in combination with 20% alginate (●), 40% alginate (▲), and 40% HPMC (◆). Tablets compressed with pure diflunisal (■).

Kinetic parameters were calculated with the aim to facilitate a rapid and easy comparison of release profiles. Dissolution efficiency (DE) is defined as the percentage of area under the dissolution curve at a fixed time. It is expressed as a percentage of the rectangular area described by 100% dissolution in the same time [30]:

$$DE = \frac{\int_0^t y \times dt}{y_{100} \times t} \times 100 \quad (3)$$

$$MDT = \frac{\sum_{j=1}^n \hat{t}_j \times \Delta M_j}{\sum_{j=1}^n M_j} \quad (4)$$

For calculating mean dissolution time (MDT), j is the sample number, \hat{t}_j is the time at the midpoint between t_j and t_{j-1} , and ΔM_j is the additional amount of drug dissolved between t_j and t_{j-1} . M_{12h} indicates the amount of drug released at a fixed time (12 h). $t_{5\%}$ indicates the time needed to release a fixed amount of drug (5%). The trends exhibited by different profiles according to the agents used can be quantified from the kinetic parameters shown in **Table 2**.

Formulation tablets	DE (%)	MDT (h)	M_{12h} (mg/mL)	$t_{5\%}$ (h)
DF-CS	94.2	0.17	64.90	<0.3
DF-CS-Alg (20%)	68.8	2.03	60.85	0.3
DF-CS-Alg (40%)	60.4	2.96	58.41	0.3
DF-CS-HPMC (40%)	31.7	8.83	34.16	0.7

Table 2. Dissolution parameters for diflunisal release from different tablets.

As can be observed, DE value closes to 100% and low mean dissolution time indicates a fast release of diflunisal from chitosan matrix causing this release that could be considered as burst-type profile. When alginate or HPMC was added to DF-CS system, a significant decrease in the dissolution rate was found, being more effective in case of HPMC as was evidenced by the low DE value and high MDT and $t_{5\%}$ values.

To test whether the addition of a higher amount of alginate results in a significant change in the rate of drug release, the comparison between different profiles can also be performed by pair-wise procedures, including difference and similarity factors (**Table 3**). The difference factor (f_1) measures the percent error between two curves over all time points, where n is the number of sampling points and R_j and T_j are the percent dissolved of the reference and test products at each time point j . Similar profiles yield f_1 values lower than 15. Similarity factors (f_2) higher than 50 indicate similar release profiles. These parameters can be calculated by the following equations:

$$f_1 = \frac{\sum_{j=1}^n |R_j - T_j|}{\sum_{j=1}^n R_j} \times 100 \quad (5)$$

$$f_2 = 50 \times \log \left\{ \left[1 + \left(\frac{1}{n} \right) \sum_{j=1}^n |R_j - T_j|^2 \right]^{-1/2} \times 100 \right\} \quad (6)$$

Profiles compared	f_1	f_2
DF-CS vs DF-CS-Alg (20%)	71	26
DF-CS-Alg (20%) vs DF-CS-Alg (40%)	13	62
DF-CS-Alg (40%) vs DF-CS-HPMC (40%)	78	19

Table 3. Comparative parameters of diflunisal release profiles.

From the data obtained for difference and similarity factors, it can be concluded that the addition of HPMC or alginate leads to different dissolution rates compared to DF-CS systems.

Different amounts of alginate (20% vs 40%) do not involve significantly changes in diflunisal release ($f_1 < 15$ and $f_2 > 50$). However, the addition of alginate and HPMC clearly proves to be significant in the dissolution rate of the drug. The different dissolution rate reduction between alginate and HPMC is also evident by comparison through f_1 and f_2 .

In the light of the different dissolution profiles shown in **Figure 12**, the study of the mechanisms involved in drug release from the different matrices is important for a better understanding of the phenomena involved in this process.

The *Korsmeyer-Peppas* equation is a simple semiempirical model which relates drug release with the elapsed time [31]. n Values indicate release exponent; for our systems, when it is close to 0.43 means that drug release occurs by pure Fickian diffusion process, when relaxation phenomena and erosion of matrix are involved in drug release, the n -value is approaching to 1. k_{KP} is a constant incorporating the structural and geometrical characteristics of the matrix system:

$$\frac{M_t}{M_\infty} = k_{KP}t^n \quad (7)$$

The *Peppas-Sahlin* model fitted to the experimental data provides values of both diffusion constant (k_D) for the Fickian contribution and erosion constant (k_E) for the erosional/relaxational contribution, the m exponent is 0.43 for our systems [32]:

$$\frac{M_t}{M_\infty} = k_D t^m + k_E t^{2m} \quad (8)$$

Kinetic fitting to aforementioned mathematical models was carried out in order to analyze the phenomena involving in drug release (**Table 4**).

Tablets	Korsmeyer-Peppas			Peppas-Sahlin ($m = 0.43$)		
	k_{KP} (h^{-n})	n	R^2	k_D (h^{-1})	k_E (h^{-1})	R^2
DF-CS	-	-	-	-	-	-
DF-CS-Alg (20%)	0.315	0.50	0.9794	0.275	0.039	0.9801
DF-CS-Alg (40%)	0.188	0.76	0.9946	0.062	0.125	0.9941
DF-CS-HPMC (40%)	0.110	0.63	0.9978	0.067	0.048	0.9986

Table 4. Kinetic constants and correlation coefficients after data fitting to Korsmeyer-Peppas and Peppas-Sahlin equations (DF-CS systems could not be fitted to kinetic equations because of the fast drug release rate corresponding to burst type).

As can be observed in the values shown in **Table 4**, a mixture of phenomena that influence drug release to the dissolution medium occurs for the systems studied (except DF-CS). In order

to assess the contribution of erosion and diffusion phenomena, erosion (E) and diffusion (D) relative contributions have been calculated [33] and represented as function of time in **Figure 13**:

$$D = \frac{1}{1 + \left(\frac{k_E}{k_D}\right)t^m} \quad (9)$$

$$1 = D + E \quad (10)$$

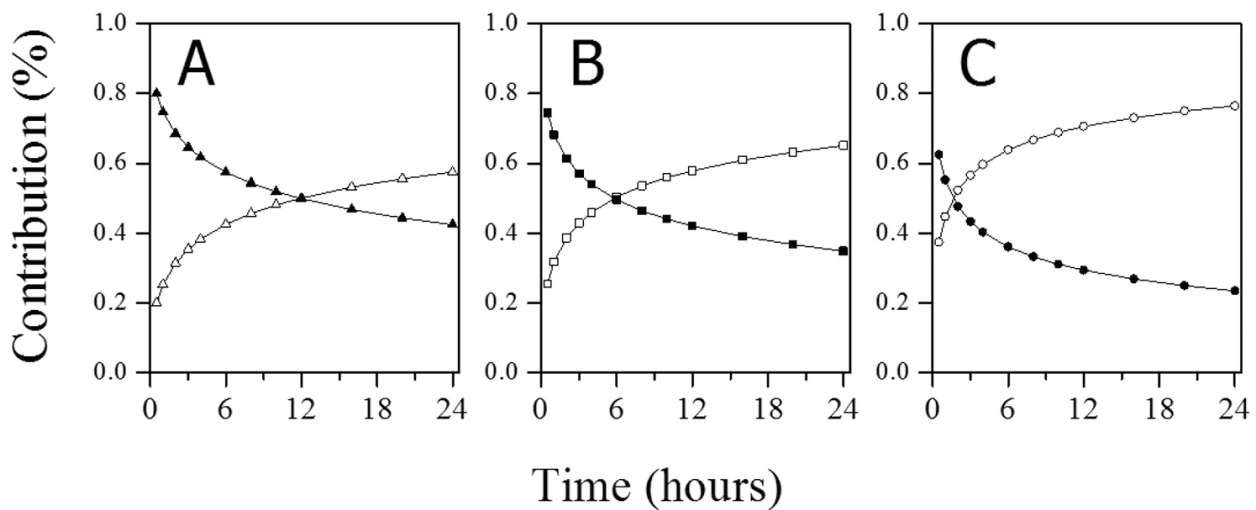


Figure 13. Erosion (empty points) and diffusion (filled points) relative contribution for DF-CS-Alg (20%) (A), DF-CS-Alg (40%) (B), and DF-CS-HPMC (40%) (C).

In all systems, the erosion contribution begins as less important than the diffusion contribution. However, this trend was inverted for the three systems. For each system a time in which the erosion is becoming more important than diffusion can be calculated. For Alg-20% system, this change occurs around 12 h while occurring at 6 h for Alg-40% system and in less than 2 h for HPMC-40% system. This contribution ratio explains why drug release from system containing HPMC is slower; in fact, the amount of drug release is practically independent of time since the erosion phenomenon reaches a greater importance than the contribution of diffusion phenomena. The same trend, but at different time, can be observed for alginate systems where the diffusion phenomenon remains longer.

3.4.2. Dissolution from nanoparticles

Diflunisal release from the previously optimized nanoparticle formulation has been studied. The same amount of diflunisal contained in nanoparticles was tested for comparison purposes. Drug dissolution profiles from nanoparticle system and pure diflunisal are shown in **Figure 14**.

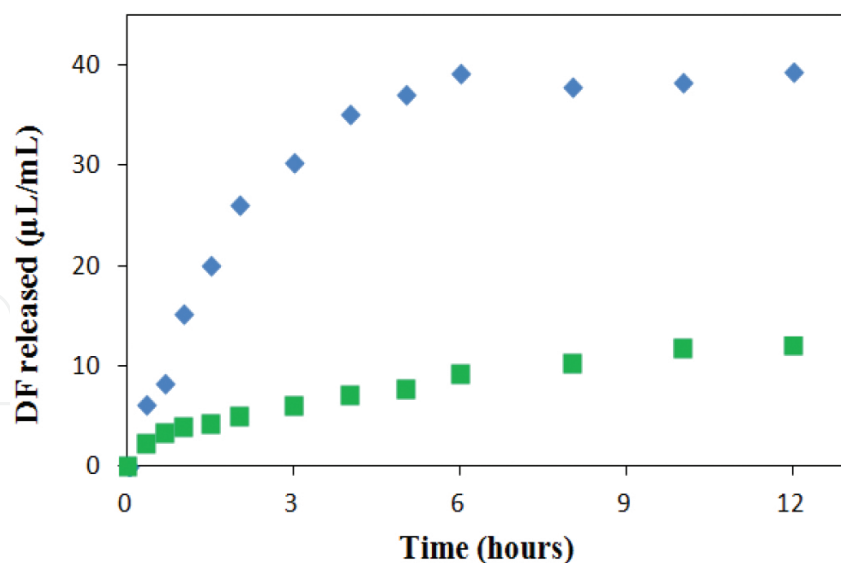


Figure 14. Dissolution rate of diflunisal from diflunisal powder (■) and CS-(DF-HP β CD) nanoparticles (◆).

Diflunisal release from nanoparticles has proven to be faster than directly from diflunisal powder. The total amount of drug encapsulated into nanoparticles was released within 6 h. However, the amount of diflunisal released in the same time is less than 10 mg/L when drug release occurs from diflunisal powder directly. This fact is due on one hand to the increase in drug solubility produced by the presence of small amounts of chitosan and HP β CD in solution; on the other hand, diflunisal molecules in nanoparticles are presented in the amorphous state, which allow to a faster release than in the case of pure diflunisal, where an additional energy is needed to break the crystal lattice.

The dissolution efficiency was 69.5% for nanoparticle system and 18.2% for pure diflunisal. This difference shows clearly a faster dissolution rate and a greater amount of drug released.

Mathematical models cannot be applied to these systems, which do not have a controlled and constant geometry that allows ascertain what proportion involved diffusion and erosion/relaxation phenomena.

4. Conclusions

Chitosan can interact with a high variety of drugs due to its physicochemical properties. The abundance and low cost associated with the production of chitosan make that it can be considered as a promising material in pharmaceutical industry. Chitosan is a versatile product able to be chemically modified and the ease to control the length of its polymer chains makes chitosan an ideal product for use in controlled release formulations.

Response surface methodology is a good tool to optimize fabrication process of pharmaceutical formulations when it depends on two or more factors. It is a good strategy to minimize the

number of experiments and to avoid mistakes usually made when the factors involved in the process are optimized individually.

The use of chitosan alone or in the presence of other excipients is made possible to obtain delivery systems on demand in solid oral dosage forms as tablets or nanoparticles. It allows us to modulate drug release from close to zero-order to type-burst kinetics.

Acknowledgements

The authors thank the University of Navarra (PIUNA project) for the financial support and the ADA for the grant of David Lucio.

Abbreviations

CS	Chitosan
DF	Diflunisal
HP β CD	2-Hydroxypropyl- β -cyclodextrin
SS	Sodium sulfate
Alg	Sodium alginate
HPMC	Hydroxypropyl methylcellulose
NPs	Nanoparticles
RSM	Response surface methodology
CCD	Central composite design
DTA	Differential thermal analysis
SEM	Scanning electron microscopy
TEM	Transmission electron microscopy
DLS	Dynamic light scattering
PDI	Polydispersity index

Author details

David Lucio* and María Cristina Martínez-Ohárriz

*Address all correspondence to: dlucio@alumni.unav.es

Department of Chemistry, Faculty of Sciences, University of Navarra, Navarra, Spain

References

- [1] Bernkop-Schnürch, A., Dünnhaupt, S. Chitosan-based drug delivery systems. *Eur. J. Pharm. Biopharm.* 81, 463–469. 2012.
- [2] Kurita, K. Chemical modifications of chitin and chitosan. In R. Muzzarelli, C. Jeuniaux & G.W. Gooday (Eds.), *Chitin in nature and technology*. (pp. 287–295) New York: Plenum. 1986.
- [3] Rinaudo, M. Chitin and chitosan: properties and applications. *Prog. Polym. Sci.* 31, 603–632. 2006.
- [4] Kato, Y., Onishi H., Machida, Y. Application of chitin and chitosan derivatives in the pharmaceutical field. *Curr. Pharm. Biotechnol.* 4, 303–309. 2003.
- [5] Domínguez-Delgado, C.L., Rodríguez-Cruz, I.M., Fuentes-Prado, E., Escobar-Chávez, J.J., Vidal-Romero, G., García-González, L., Puente-Lee, R.I. Drug carrier systems using chitosan for non-parenteral routes. *Pharmacology and Therapeutics.* 273–325. 2014
- [6] He, W., Guo, X., Xiao, L., Feng, M. Study on the mechanisms of chitosan and its derivatives used as transdermal penetration enhancers. *Int. J. Pharm.* 457, 158–167. 2009.
- [7] Sinha, V.R., Singla, A.K., Wadhawan, S., Kaushik, R., Kumria, R., Bansal, K., Dhawan, S. Chitosan microspheres as a potential carrier for drugs. *Int. J. Pharm.* 274, 1–33. 2004.
- [8] Hillyard, I.W., Doczi, J., Kiernan, P.B. Antacid and antiulcer properties of the polysaccharide Chitosan in the rat. *Exp. Biol. Med.* 115, 1108–1112. 1964.
- [9] Acikgoz, M., Kas, H.S., Hascelik, Z., Milli, Ü., Hincal, A.A. Chitosan microspheres of diclofenac sodium, II: in vivo and in vitro evaluation. *Pharmazie.* 117, 41–48. 1995.
- [10] García Mir, V., Heinämäki, J., Antikainen, O., Sandler, N., Bilbao Revoredo, O., Iraizoz Colarte, A., Nieto, O.M., Yliruusi, J. Application of crustacean chitin as a co-diluent in direct compression of tablets. *Pharm. Sci. Technol.* 11, 409–415. 2010.
- [11] Prabakaran, M. Chitosan derivatives as promising materials for controlled drug delivery. *J. Biomater. Appl.* 23, 5–36. 2008.
- [12] Zhou, X., Hu, Y., Tian, Y., Hu, X. Effect of N-trimethyl chitosan enhancing the dissolution properties of the lipophilic drug cyclosporine A. *Carbohydr. Polym.* 76, 285–290. 2009
- [13] Uragami, T., Tokura, S. *Material Science of chitin and Chitosan*. Tokyo: Kodansha. 2006.
- [14] Riva, R., Ragelle, H., des Rieux, A., Duhem, N., Jérôme, C., Prétat, V. Chitosan and chitosan derivatives in drug delivery and tissue engineering. In *Chitosan for biomaterials II* (pp. 19–44). Springer, Berlin Heidelberg. 2011.

- [15] Sugimoto, M., Morimoto, M., Sashiwa, H., Saimoto, H., Shigemasa, Y. Preparation and characterization of water-soluble chitin and chitosan derivatives. *Carbohydr. Polym.* 36, 49–59. 1998.
- [16] Lu, G., Kong, L., Sheng, B., Wang, B., Gong, Y., Zhang, X. Degradation of covalently cross-linked carboxymethyl chitosan and its potential application for peripheral nerve regeneration. *Eur. Polym. J.* 43, 3807–3818. 2007.
- [17] Aiping, Z., Wenjie, J., Lanhua, Y., Gongjun, Y., Hui, Y., Hao, W. O-Carboxymethylchitosan-based novel gatifloxacin delivery system. *Carbohydr. Polym.* 68, 693–700. 2007
- [18] Lucio, D., Irache, J.M., Martínez-Ohárriz, M.C., Response surface methodology for optimization of chitosan coated nanoparticles. 19th International Symposium on Microencapsulation, Pamplona, September 2013. pp 64.
- [19] Lucio, D., Zornoza, A., Martínez-Ohárriz, M.C. Influence of chitosan and carboxymethylchitosan on the polymorphism and solubilisation of diflunisal. *Int. J. Pharm.* 467(1), 19–26. 2014.
- [20] Sarabia, L.A., Ortiz, M.C. Response surface methodology. *Compr. Chemom.* 1, 345–390. 2009.
- [21] Martínez-Ohárriz, M.C., Martín, C., Goñi, M.M., Rodriguez-Espinosa, C., Tros-Illarduya, M.C., Zornoza, A. Influence of polyethylene glycol 4000 on the polymorphic forms of diflunisal. *Eur. J. Pharm. Sci.* 8, 127–132. 1999.
- [22] Martínez-Ohárriz, M.C., Rodriguez-Espinosa, C., Martín, C., Goñi, M.M., Tros-Illarduya, M.C., Sánchez, M. Solid dispersions of diflunisal-PVP: polymorphic and amorphous states of the drug. *Drug Dev. Ind. Pharm.* 28, 717–725. 2002.
- [23] Agüeros, M., Zabaleta, V., Espuelas, S., Campanero, M.A., Irache, J.M. Increased oral bioavailability of paclitaxel by its encapsulation through complex formation with cyclodextrins in poly (anhydride) nanoparticles. *J. Controlled Release*, 145(1), 2–8. 2010.
- [24] Zornoza, A., Sánchez, M., Vélaz, I., Fernández, L. Diflunisal and its complexation with cyclodextrins. A fluorimetric study. *Biomed. Chromatogr.* 13, 111–112. 1999.
- [25] Zugasti, M.E., Zornoza, A., Goñi, M.M., Isasi, J.R., Vélaz, I., Martín, C., Sánchez, M., Martínez-Ohárriz, M.C. Influence of soluble and insoluble cyclodextrin polymers on drug release from hydroxypropyl methylcellulose tablets. *Drug Dev. Ind. Pharm.* 35, 1264–1270. 2009.
- [26] Tempero, K.F., Cirillo, V.J., Steelman, S.L. Diflunisal: a review of pharmacokinetic and pharmacodynamic properties, drug interactions, and special tolerability studies in humans. *Br. J. Clin. Pharmacol.* 4(S1), 31S–36S. 1977.
- [27] Agnihotri, S.A., Mallikarjuna, N.N., Aminabhavi, T.M. Recent advances on chitosan-based micro-and nanoparticles in drug delivery. *J. Controlled Release*, 100(1), 5–28. 2004.

- [28] Cotton, M., Hux, R. Diflunisal. In K. Florey (Ed.), *Analytical profiles of drug substances*. (pp. 491–526) London: Academic Press Inc. 1985.
- [29] Martínez-Ohárriz, M.C., Martín, C., Goñi, M.M., Rodríguez-Espinosa, C., Troslarduya, M.C., Zornoza, A. Polymorphism of diflunisal: isolation and solid-state characteristics of a new crystal form. *J. Pharm. Sci.* 83, 174–177. 1994.
- [30] Costa, P., Sousa Lobo, J.M. Modeling and comparison of dissolution profiles. *Eur. J. Pharm. Sci.* 13, 123–133. 2001.
- [31] Korsmeyer, R.W., Gurny, R., Doelker, E., Buri, P., Peppas, N.A. Mechanism of solute release from porous hydrophilic polymers. *Int. J. Pharm.* 15, 25–35. 1983.
- [32] Peppas, N.A., Sahlin, J.J. A simple equation for the description of solute release. III Coupling of diffusion and relaxation. *Int. J. Pharm.* 57, 169–172. 1989.
- [33] Sujja-areevath, J., Munday, D.L., Cox, P.J., Khan, K.A. Relationship between swelling, erosion and drug release in hydrophilic natural gum mini-matrix formulations. *Eur. J. Pharm. Sci.* 6, 207–217. 1998.

